



Mechanical Engineering

Elixir Mech. Engg. 75 (2014) 27388-27396

Elixir
ISSN: 2229-712X

The Flexing Fatigue Properties of Filled Rubbery Compounds under Constant and Variable Amplitude Loading

Hussain J.M. Al-Alkawi¹, Dhafir S. Al-Fattal² and Nabel K. Abd-Ali³

¹Electromechanical Engineering Department, University of Technology, Baghdad- Iraq.

²Mechanical Engineering Department, University of Technology, Baghdad- Iraq.

³College of Engineering, Al-Qadisiya University, Al-Dewaniya City- Iraq.

ARTICLE INFO

Article history:

Received: 15 January 2013;

Received in revised form:

20 September 2014;

Accepted: 29 September 2014;

Keywords

Crack growth,
Rubber,
Sidewall,
Flexing, Paris law,
Accumulative fatigue,
Miner Rule.

ABSTRACT

Crack growth characteristics of rubbery materials are an important factor in determining the strength and durability of the materials. The present work studied three stocks composed of Natural Rubber (NR), Styrene Butadiene Rubber (SBR) and Polybutadiene Rubber (BR_{cis}) filled with carbon black N330. Three percentages of (NR/SBR/BR_{cis}) were studied, namely (40/60/0), (40/50/10) and (40/40/20). The intent was to develop the Standard Italian Perilli Recipe (SPR) for Truck Tires Sidewall manufactured in Al-Dewaniya Tires Factory that have (30NR/70SBR) filled with carbon black N550. The results of constant amplitude loading have verified the applicability of the Paris law to the flexing fatigue behaviour of truck tire sidewall components. The accumulative fatigue damage was studied by the application of Miner's rule to variable amplitude loading and gave unacceptable safe results at both sequence (L-H) and (H-L). The recipe that has (NR/SBR/BR_{cis}) blending with percentages of (40/50/10) was generally the best in combined properties.

© 2014 Elixir All rights reserved

Introduction

The ability of rubber to withstand very large strains with out permanent deformation makes it ideal for many applications such as tires, vibration isolators, seals, hoses and belts. As these applications impose large static and time-varying strains, durability and therefore mechanical fatigue is often the primary consideration. Such tools have been developed for other materials. However, these are commonly based upon theories of material behaviour that cannot be applied to rubber, due to rubber's highly deformable and nonlinear nature. Typically, the fatigue failure process involves a period during which cracks nucleate in critical regions that were initially free of observed cracks, followed by a period of crack growth to the point of failure [1-3].

Mars and Fatemi [4] reported that many factors influence the fatigue behaviour of rubber. They include various aspects of the mechanical loading history, environmental effects, effects of rubber formulation and effects due to the dissipative aspects of the constitutive response of rubber. A primary consideration relating to the mechanical load history is rubber's extreme sensitivity to not only the load range, but also the R ratio. Depending on the polymer type and the presence of fillers, the effect of increasing the minimum or mean loading may be either beneficial or harmful [1-3]. It was also reported that the fatigue life initiation and propagation in natural and synthetic rubbers are dependent upon the chemical composition, environment and the mechanical stresses applied to the sample [5].

Strain-crystallizing rubbers such as natural rubber were shown to be very sensitive to changes in the R-ratio as the fatigue crack growth rates drastically dropped for natural rubber as the minimum stress level was gradually increased. This sensitivity to R-ratio was not present during tests performed on SBR, which does not strain-crystallize. A small minimum stress

level can yield very beneficial effects to the fatigue crack growth behavior [6].

Fatigue Crack Growth (FCG) Behavior:

The most commonly used crack growth parameter for rubber is the energy release rate or tearing energy. This concept is based on the idea that crack growth is due to the conversion of stored potential energy to surface energy related to new crack surfaces. Measurements of the crack growth behavior under repeated stressing using various test pieces may be expressed as the crack growth per cycle (dc/dN) as a function of G or K . Results for a natural rubber (NR) compound indicate that the crack growth under repeated stressing is independent of the test piece geometry, hence, it is a true strength property of the material, and a logarithmic plot holds [7-11]:

$$da/dN = BG^a \dots\dots\dots(1)$$

where a is the crack length, N is the number of load applications (cycles), and $(B \text{ and } \alpha)$ are material constants.

Crack growth is predicted by the calculation of the tearing energy for given specimen under prescribed loading conditions. It is well-adapted to tires problem in which the parts should be able to sustain crack propagation before failure [12,13].

The scientific basis for the optimization of fatigue life is to determine the rate of fatigue crack growth over a broad range of tearing energies. In practice, rubber products usually meet with progressive weakening of mechanical properties, and finally reach failure due to mechanical fatigue, i.e. continual crack growth under sinusoidal excitation with an extended period of time. The crack growth characteristics of rubbery materials must be, therefore, an important factor determining their strength and durability [14]. The fatigue crack growth is affected by not only material variables such as rubber type, but also test conditions such as test frequency, temperature and strain amplitude [15,16].

Thus the crack growth properties of rubber are important in deciding its strength [11]. Fatigue crack growth rate of elastomers and the effect of various factors like frequency, temperature, fillers and ozone were studied previously [17-19]. Frank [20] described the fatigue life and dynamic crack propagation behaviour of elastomers, especially their dependency on test parameters. Tests were made in order to create a common Wohler-(S-N)-curve while increasing stress amplitude. The influence on fatigue properties of increasing minimum stress at constant stress amplitude was investigated. The investigation shows that the fatigue behaviour of carbon black filled non strain crystallizing rubbers can't be described with a maximum stress or a maximum strain criterion. It shows that an energy criterion should be considered.

Thomas [21] found that if a NR test piece containing a crack is repeatedly loaded and unloaded, then there is an increment in crack length for each loading cycle. The extent of rupture can perhaps be reduced by the redistribution of the local stresses by strain-induced crystallization; more rupture could occur on a subsequent loading before crystallization again occurs [22]. Lindley [23] carried out crack-growth tests of NR under non-relaxing cyclic conditions, and found that the rate of crack growth was retarded compared to relaxing load cycles, the greater the minimum energy release rate the greater the retardation. Similar results are well known for fatigue of NR (e.g. [24]).

An alternate analysis for fatigue crack growth is based on stress intensity factor (SIF) and involves the use of Paris law. While the Paris law is widely accepted in classical fracture mechanics, its application to elastomeric materials has been debated. However, it may shed light on the mechanics of failure in this analysis. For an applied load that is cycled uniformly between K_{max} and K_{min} , the Paris Law relation is given by [25,26]:

$$\frac{da}{dN} = A(\Delta K)^\alpha \quad \dots \dots \dots (2)$$

where A and α are material constants, and

$$\Delta K = K_{max} - K_{min} \quad \dots \dots \dots (3)$$

where ΔK is the stress intensity factor range.

The Paris law is suited for non-relaxing fatigue tests because it deals with the stress intensity factor range (ΔK), where the assumption is made that the stress is never returned to zero during the fatigue cycle. In the analysis, the relevance of the Paris law to fatigue testing of a natural rubber compound will be determined. Calculating the stress intensity factor K_I at a crack tip involves the length of the crack, the stress in the material. Therefore, at a given crack length the stress intensity factor at a crack tip is directly proportional to the stress level in the test specimen [26]. As in present work, most studies considered the prediction of the fatigue crack growth rate is only whilst the crack is advancing in a broadly straight line [27].

Prediction of Fatigue Life:

The prediction of fatigue life in elastomer materials involved application of a fracture mechanics method on simple geometries was studied previously and proved that fatigue crack growth can be predicted by the application of fracture mechanics with a high degree of accuracy, and could prove to be a good tool for fatigue crack growth problems since it deals with material properties rather than geometric properties and loading conditions [28].

In the case of tyres, where failure can be disastrous, the typical failure mode involves the growth of cracks in the body of the tyre, typically from cyclic flexing of the sidewall,

damage due to repeated cutting or just the surface abrasion process.

The fatigue life of the material can be calculated using following equation [29]:

$$N_f = \int_{a_0}^{a_c} \frac{da}{A(\Delta K)^\alpha} \quad \dots \dots \dots (4)$$

where,

a_0 , a_c : the initial and final crack length.

Cumulative Fatigue Damage:

Service load histories for engineering applications are usually variable amplitude, whereas the stress-life approach outlined is only applicable for constant amplitude loading. Cumulative damage under spectrum loading is evaluated by taking into account the cyclic stress amplitude, the number of cycles of operation at that stress amplitude, and also the total number of cycles of life of an undamaged specimen at that stress amplitude. The damage incurred is considered permanent, and operation at several different stress amplitudes in sequence will result in an accumulation of total damage equal to the sum of the damage increments accrued at each individual stress level. When the total accumulated damage reaches a critical value, fatigue failure is predicted to occur [30].

The linear damage rule by Palmgren and Miner is widely used because of its simplicity. The assumption here is that the damage accumulation is linear. The general form of the Palmgren-Miner rule [35] is given by:

$$\sum_{i=1}^m \left(\frac{n_i}{N_i} \right) = 1 \quad \dots \dots \dots (5)$$

where m = number of stress levels in the block loading spectrum, n_i = number of cycles at each stress level in the block loading spectrum and N_i = number of cycles to failure at each stress level.

Sun et al.[31] studied the effects of applying step-up and step-down sequences of strains on residual ultimate tensile strengths in typical filled tire compounds. The purpose of the study was to evaluate the suitability of Miner's linear damage rule for the development of accelerated tire durability tests. Miner's rule predicts no dependence on loading sequence. The study found that "in all cases, a series of increasing strains reduced the strength to a greater degree than the same strains applied in decreasing order." This effect is attributed to a strain-dependent Paris-law exponent, and to the effect of stress-softening.

The aim of this practical work is to understand the crack growth behaviour under constant and variable amplitude loading as a function of the stress intensity factor (SIF) and flex times (cycles) correlated to understand the performance of a model truck tire sidewall and acceptability of Paris law. Also, a comparison of experimental life ($N_{f_{exper.}}$) with Miner rule calculations ($N_{f_{Miner}}$) is carried out.

Experimental Work:

The sidewall component of a tire is an important part and amount up to 20 percent of the whole tire by weight. Based on tire structure and its practical use, sidewall properties should be relevant to Dewaniya Tires Factory conditions (according to Perilli Co.) with several requirements such as flex life, tensile strength, tear strength, compressive strength, crack-growth resistance, and gloss surface.

Materials:

In the present work, Natural Rubber (NR), Styrene Butadiene Rubber (SBR) and Polybutadiene Rubber (BR_{cis}) were used to investigate the effect of blends in different percentages on the characteristics and mechanical properties of

rubber compounds. The materials used in this study to prepare the rubber compounds were Elastomers (Natural Rubber (SVR5), Synthetic Rubber SBR and BR_{cis}), Fillers (Carbon Black FEF N330, with 51 pphr), Antioxidants (TMQ, with 1 pphr), Anti-ozonants (IPPD with 1.75 pphr and paraffin wax with 3 pphr), Accelerators (CBS with 0.5 pphr), Activators (Zink oxide with 4 pphr, Stearic acid with 2 pphr), Softening Aids (Dutrex Oil, with 8.5 pphr) and Vulcanizing Agents (Sulfur, with 2 pphr). The mixing conditions and procedure were made at a temperature of 70 ± 5 °C (158 ± 9 F), mixing speed (slow roll) 24 rpm and roll ratio of slow to fast roll (1 to 1.4). Table (1) shows the stocks percentages that were used during the present work. More details about these stocks can be found elsewhere [32].

Table (1): Rubber Percentage (pphr)

stock	NR	SBR	BR _{cis}
SPR	70	30	--
J	40	60	--
K	40	50	10
L	40	40	20

Mechanical and Physical Tests:

Tensile Test: Test method for Dumbbell shape specimen was used and the test was controlled at room temperature ($23-25$ °C) and at loading rate 500 mm/min with uniform thickness. The machine used was Monsanto T10 Tensometer and according to ASTM D412 [33].

Tear Test: A tearing strain (and stress) is applied to a test specimen by means of a tensile testing machine operated without interruption at a constant rate until the specimen is completely torn. This test method measures the force per unit thickness required to rupture, initiate, or propagate a tear through a sheet of rubber in the form of one of several test piece geometries. The testing machine shall conform to the requirements as specified in Test Method D412. The rate of jaw separation shall be 500 mm/min (20in./min.) according to ASTM D624, Type B[34]. Fig.(1) shows the Monsanto Tensometer for tensile and tear tests.



Fig.(1): Monsanto T10 Tensometer.

Fatigue (Cut Growth) Test: This test method covers the determination of crack growth of vulcanized rubber when subjected to repeated bending strain or flexing at 5Hz and 60 ± 2 °C. It is particularly applicable to tests of synthetic rubber compounds which resist the initiation of cracking due to flexing when tested according to ASTM D813 and method B of Test Methods ASTM D430 [35, 36]. The De Mattia flexing machine and Flexing Specimen are shown in fig.(2). Final failure is considered at (Grade 10) where the length of the largest crack is greater than 15.00 mm. More details about the test method can be found elsewhere [37].



Fig.(2): De Mattia Flexing Machine Test

Results and Discussion

Table (2) shows the mechanical properties for 3 stocks in addition to the base rubber stock (SPR) or stock 1.

Table (2): Mechanical Properties of Recipes.

Stock	Ten. Str. (MPa)	Modulus at 300%	Elong. at Break (%)	Tensile Improv. (%)
1	15.10	9.56	408.30	--
A	19.11	15.12	391.33	26.55
B	17.77	14.13	389.67	17.68
C	18.13	13.44	398.61	20.1

Table (3) shows the tear strength for three stocks in addition to the Standard Perilli Recipe (SPR), stock 1.

Table (3): Tear Strength Data.

Stock	Tear Strength (MPa)	Improvement (%)
SPR	3.10	--
A	6.67	115.16
B	6.68	115.48
C	6.47	108.71

These results were discussed in previous works for the same authors including the effect of rubber type and carbon black type, where these stocks were selected as the best recipes for truck tire sidewall. More details can be found elsewhere [32,37].

Flexing Fatigue at Constant Amplitude Loading(CAL):

The cyclic loading components with CAL are assumed to simplify the analysis. Fig.(3) shows fatigue test specimen under zero tension and region X.



Fig.(3): Fatigue Test Specimen under Zero Tension

Fig.(4) shows same specimen under 50 mm tension (1.82 MPa).

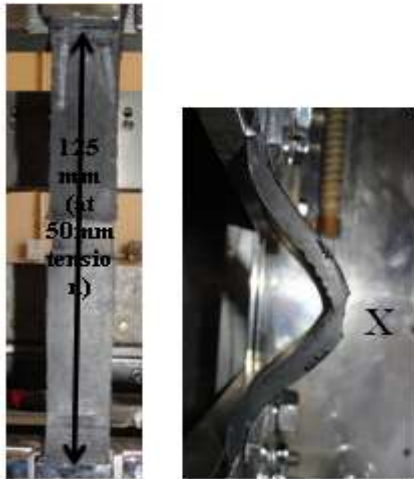


Figure (4): Fatigue Test Specimen under (50 mm) Tension
Table (4) reports the stresses in each state of tension and compression in addition to the change in effective radiusing in grooving of strip specimen test X at tension and compression state.

Table (4): Stresses and Dimension of Groove X.

Tension (mm)	Stress (MPa)		Dimension of Groove X	
	tension	compression	tension	compression
0	0	0.24	5	11
30	1.45	0.13	10.37	10.51
50	1.8	0.1	11.68	9.22

The crystalline domains of NR imparts the green strength and gives vulcanized rubber high cut growth resistance at severe deformation even without reinforcement, and BR_{cis} are used in blend with NR and SBR to achieve techno-economic benefits, and improves flex cracking and fatigue resistance[38-41].

For a non-crystallizing elastomer such as SBR and BR_{cis}, the fatigue life is much more dependent on the size of the initial flaw, and the magnitude of the imposed deformation. Such elastomers are generally longer-lived at small deformations, but much shorter-lived under more severe conditions. The fatigue life is also drastically lowered at high temperatures as a result of the sharp increase in cut growth rate as the internal viscosity is decreased [26], i.e. the difference between standard stock and new recipes is the range of (NR/SBR) from 10-30 pphr, which may have caused the improvements of some of the results. BR_{cis} shows low hysteresis combined with good wear characteristics [42]. When blended with other synthetic rubbers such as SBR, it combines BR properties with malleability and extrudability [38,43].

Figure (5) shows the crack growth increment after the first 300cycle and at every 1000 cycle under 30 mm tension, where the cut growth rate of the stocks A and C were smaller compared with the standard stock, and the best results here are for the stock B.

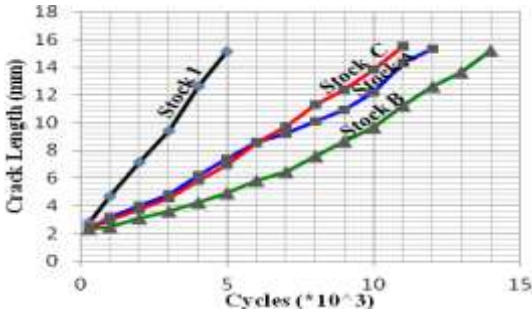


Figure (5): Crack Length vs. Cycles at Constant load at 30 mm tension

Figure (6) shows the crack growth increment under 50 mm tension the trend for the different stocks is similar to that shown in figure (5-40), but the life decreases.

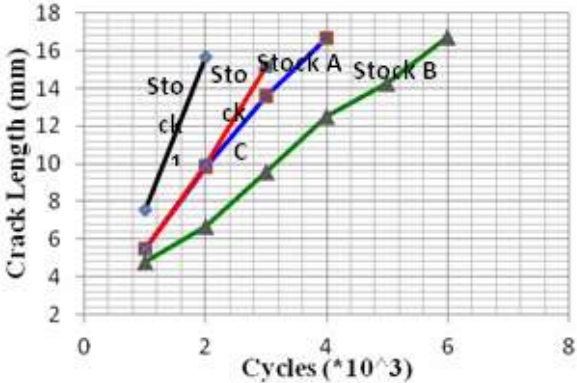


Figure (6): Crack Length vs. Cycles at Constant load at 50 mm tension

The flex-cracking behaviour of NR is better than SBR at higher strains and therefore, sidewalls of radial tyres incorporate substantial proportions of NR [44].The above improvement may be related to the increase in NR percentage and the use of BR_{cis}.

Elevated temperature has a deleterious effect on fatigue crack growth rate of rubber. Temperature has a large effect on the rate of these chemical processes, which can result in additional degradation of fatigue life at elevated temperatures, or over long periods [4]. Joseph and Ioannis report that the fatigue life decreases with increasing testing temperature [5,27].

The same relationship between crack growth increments versus cycles has been previously documented [1,26,27,45]. Lake and Lindley [45] reported that the rate of crack growth that arose from a sharp cut during the first few cycles was substantially quicker than the steady state rate measured after a few hundred cycles. Ioannis [27] illustrated the relationship between crack length versus number of cycles for gearbox mount under dynamic tensile loading under (10 mm, 14 mm and 16 mm), the present work is compared with these results as shown in figure (7). The trend of the present results is similar to those reported.

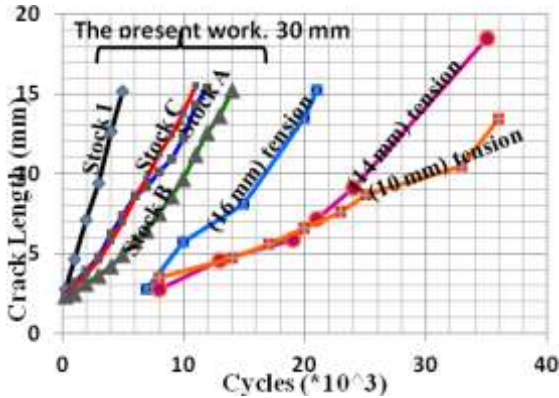
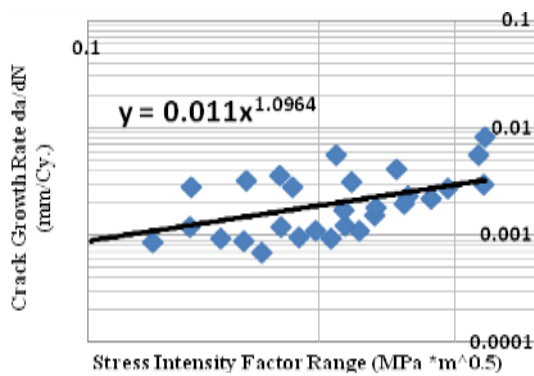
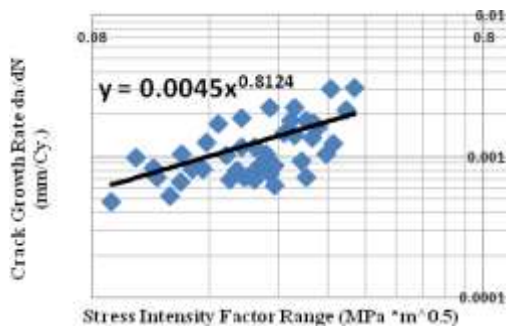
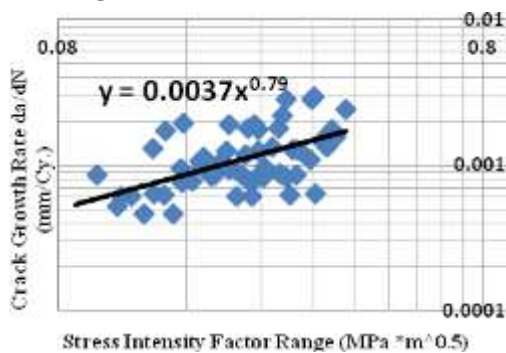
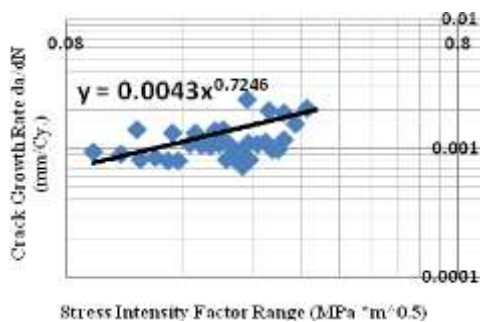
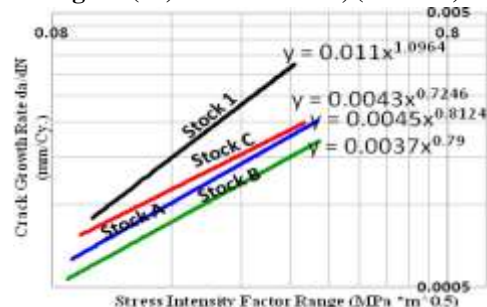


Figure (7): Crack Length vs. Cycles, Comparison with Ioannis Results [9]

Crack Growth and Stress Intensity Factor Relationship
The Paris law and tearing energy relationships are similar in that they both are based on a power law equation. The Paris law is different however because it explicitly takes into account the non-relaxing characteristic of a fatigue cycle [26].

Figures (8), (9), (10) and (11) shows the plot of fatigue crack growth rate FCG (da/dN) as a function of stress intensity factor range (SIF) or ΔK for the stocks 1, 16, 19 and 22 respectively. Also figure (12) shows the final results for these stocks.

Figure (8): da/dN vs. ΔK , (Stock 1).Figure (9): da/dN vs. ΔK , (Stock A).Figure (10): da/dN vs. ΔK , (Stock B).Figure (11): da/dN vs. ΔK , (Stock C).Figure (12): $\left(\frac{da}{dN}\right)$ vs. (ΔK) All Stocks.

The crack growth rate, dc/dN was calculated at each specific Range of stress intensity factor ΔK . All the different rates are shown in Figures using a log-log plot of dc/dN in (mm/Cy.), versus ΔK in (MPa \sqrt{m}). It can be concluded that the FCG rate increases with increasing crack length where it is a continuous incremental relationship until failure. From the sets of experimental data, the values of the coefficient (A) and exponent (α) of these stocks in the Paris law takes the form:

$$\text{stock 1} \quad \frac{da}{dN} = 11 * 10^{-3} (\Delta K)^{1.0964} \dots \dots \dots (6)$$

$$\text{stock A} \quad \frac{da}{dN} = 4.5 * 10^{-3} (\Delta K)^{0.8124} \dots \dots \dots (7)$$

$$\text{stock B} \quad \frac{da}{dN} = 3.7 * 10^{-3} (\Delta K)^{0.79} \dots \dots \dots (8)$$

$$\text{stock C} \quad \frac{da}{dN} = 4.3 * 10^{-3} (\Delta K)^{0.7246} \dots \dots \dots (9)$$

The crack of stock B increases more slowly than other stocks under the same conditions. Whether or not the polymer exhibits strain crystallization is a primary consideration. From Lake and Lindley's results for fatigue crack growth behavior, it can be seen that rubbers that exhibit strain crystallization have a lower fatigue crack growth. BR also exhibits superior performance at low energy release rates [4]. Styrene-butadiene (SBR) does not exhibit strain crystallization, and has therefore worse wear resistance as compared to natural rubber [9]. Young's results show that the power-law exponent on energy release rate can be controlled somewhat by blending of different polymer types [4].

The same relationship between crack growth increments versus cycles has been previously documented [5,9,26]. Joseph [5] reported that increasing temperatures generally increase the slope of the fatigue crack growth but this increase in the slope can vary greatly between different elastomers e.g. natural rubber (NR), styrene butadiene rubber (SBR) and butadiene rubber (BR). Both NR and BR showed little strain rate dependency. Bathias and Legorju [46] demonstrated that damage due to chemical effects is greater at higher temperatures due to the acceleration of the oxidation reaction.

Schubel et al [26] illustrate the plot of crack growth rate as a function of ΔKI . The data points fall on a straight line, with slightly more scatter towards the lower ΔKI values, where Paris law takes the form:

$$\frac{da}{dN} = 6.9 * 10^{-2} (\Delta K)^{0.211} \dots \dots \dots (10)$$

Crack Growth and Life Relationship:

From the present work the integration of power law gives:

$$N_f = \frac{1}{\left(1 - \frac{\alpha}{2}\right) * A * (\sigma * \sqrt{\pi})^\alpha} \left[a_c^{\left(1 - \frac{\alpha}{2}\right)} - a_o^{\left(1 - \frac{\alpha}{2}\right)} \right] \dots (11)$$

where a_o, a_c : initial and critical crack length, here equal to (2 and 15mm) respectively.

Schubel et al [26] report that the life can calculate from:

$$N_f = \frac{1}{(\beta - 1)B(2kw)^\beta (a_o^{\beta-1} - a_c^{\beta-1})} \dots (12)$$

where B and β represent material constants, and 2kwa represent the energy release rate [26,47];

Figure (13) shows the stress- life relationship where stock B have the best results compared with other stocks.

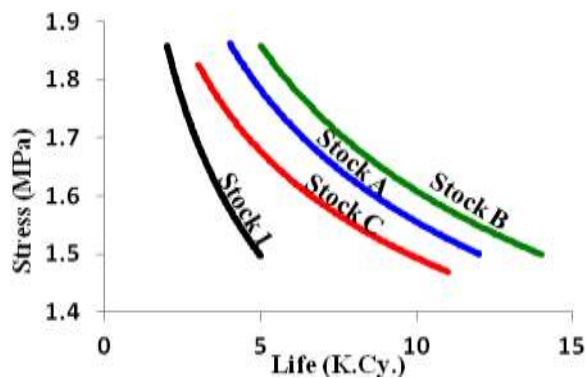


Figure (13): Stress vs. Life.

Flexing at Variable Amplitude Loading (VAL):

Variable amplitude test signals were selected to simulate some common aspects from actual load histories. Table (5) shows the life under constant amplitude loading that was used as a base for cumulative damage calculations under 30mm and 50mm tension.

Table (5): Life at Constant Amplitude Loading.

Stock	N_f at 30 mm tension (Cycle)	N_f at 50 mm tension (Cycle)
1	5000	2000
A	12000	4000
B	14000	5000
C	11000	3000

Accumulative Fatigue Damage at (Low-High) Sequence:

Figure (14) shows Terminology used in Variable Amplitude Loading (L-H) sequence.

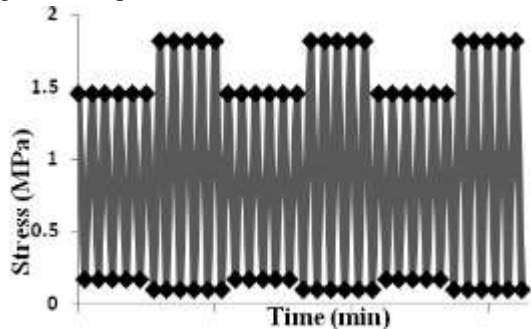


Figure (14): Low-High Sequence.

Figure (15) shows the crack growth increment after the first 300 cycle and at every 1000 cycle under (L-H) sequence, where the cut growth rate of the stocks A and C still smaller compared with the standard stock, and the best results here are for the stock B too.

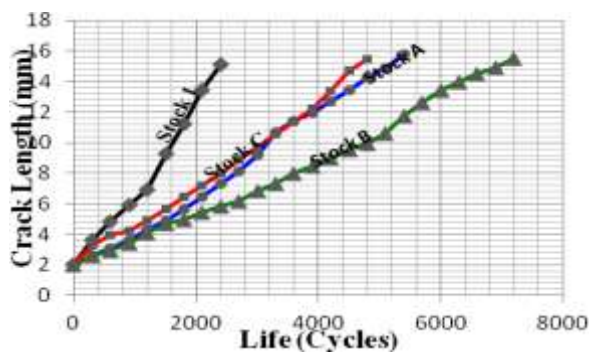


Figure (15): Crack Length vs. Life, (L-H) Sequence.

Figures (16), (17), (18) and (19) shows the plot of fatigue crack growth rate FCG (da/dN) as a function of stress intensity factor range ΔK for the stocks 1, A, B and C respectively.

Also figure (20) shows the final results for these stocks under (L-H) sequence.

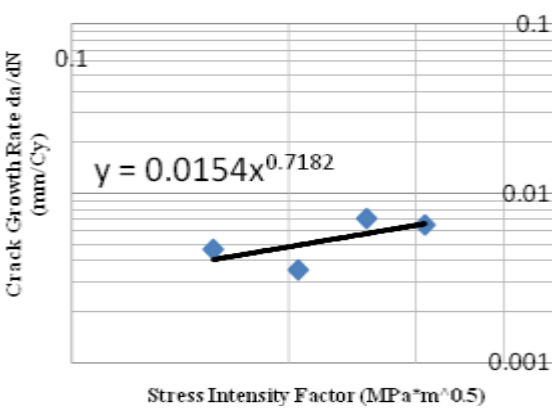


Figure (16): da/dN vs. ΔK , (Stock 1).

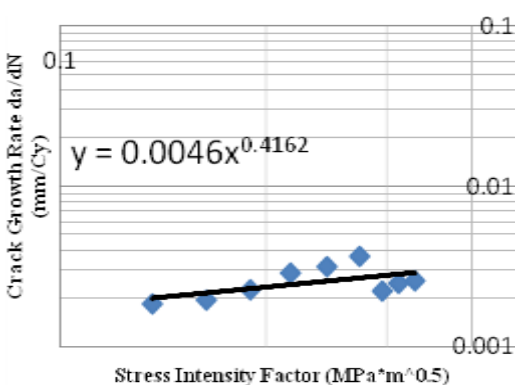


Figure (17): da/dN vs. ΔK , (Stock A).

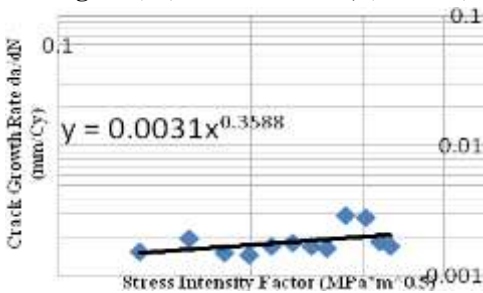


Figure (18): da/dN vs. ΔK , (Stock B).

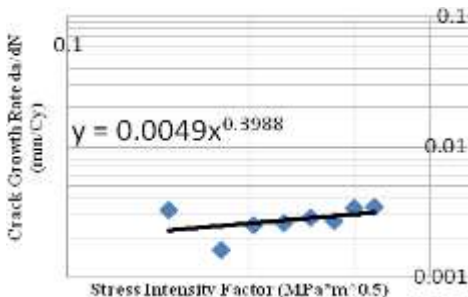


Figure (19): da/dN vs. ΔK , (Stock C).

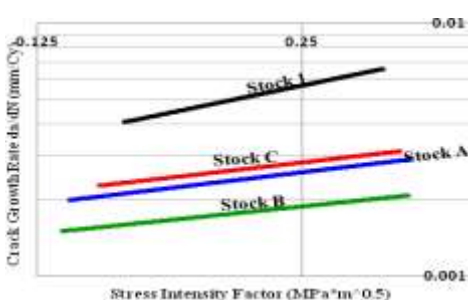


Figure (20): da/dN vs. ΔK , All Stocks.

From the sets of experimental data, the values of the coefficient (A) and exponent (α) of these stocks in the Paris law takes the form:

stock 1
$$\frac{da}{dN} = 15.4 * 10^{-3} (\Delta K)^{0.7182} \dots (13)$$

stock A
$$\frac{da}{dN} = 4.6 * 10^{-3} (\Delta K)^{0.4162} \dots (14)$$

stock B
$$\frac{da}{dN} = 3.1 * 10^{-3} (\Delta K)^{0.3588} \dots (15)$$

stock C
$$\frac{da}{dN} = 4.9 * 10^{-3} (\Delta K)^{0.3988} \dots (16)$$

These results may be related to the same reasons that mentioned previously with the same stocks under constant amplitude load where stock B was the best. Table (6) shows the Miner life Nf_{Miner} , experimental life Nf_{exp} .

Table (6): Accumulative Fatigue Damage Results (L-H) Sequence.

Stock	Nf_{Miner} (Cycle)	$Nf_{Exp.}$ (Cycle)
1	2857	2400
A	6000	5400
B	7368	7200
C	4714	4800

Nf_{miner} calculated from:

$$\sum \frac{n}{N_{f\sigma_L}} = D \dots (17)$$

And according to Miner $D=1$, and at $n = 300$

$$\left(\frac{n}{N_{f\sigma_L}} + \frac{n}{N_{f\sigma_H}} \right) * X_{miner} = D_{miner} \dots (18)$$

$N_{f\sigma_L}, N_{f\sigma_H}$ the number of fatigue cycle to failure at constant stress at low and high stresses Respectively.

$$N_{f_{Miner}} = \frac{2nX_{miner}}{D_{miner}} \dots (19)$$

The experimental life results from the variable amplitude loading showed that at (L-H) sequence the results of Miner's Rule were not acceptable, where it seem not safe because the Nf_{Miner} was larger than the Nf_{exp} . Stock C only have unpretending safety factor about (1.8), while in the practice we need safety factor about (3) to work with these compound such as that suggested in previous study during with sidewall and tread recipes to assurance the work with Miner rule at this sequence [48]. The using of Miner's rule with (L-H) sequence in flexing fatigue conditioned with using of acceptable safety factor.

Accumulative Fatigue Damage at (High-Low) Sequence:

Figure (21) shows Terminology used in variable amplitude loading at (H-L) sequence.

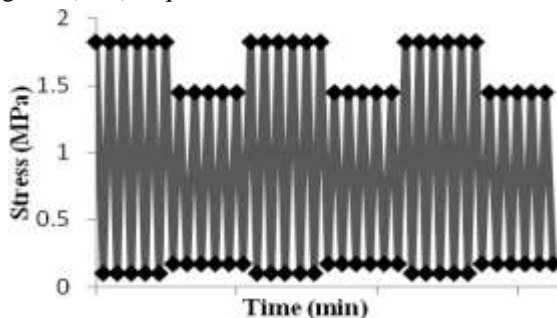


Figure (21): High-Low Sequence.

Figure (22) shows the crack length after the first 300 cycle and at every 1000 cycle under (H-L) sequence, where the cut

growth rate of the stocks A and C still smaller compared with the standard stock and the best results here are for the stock B too.

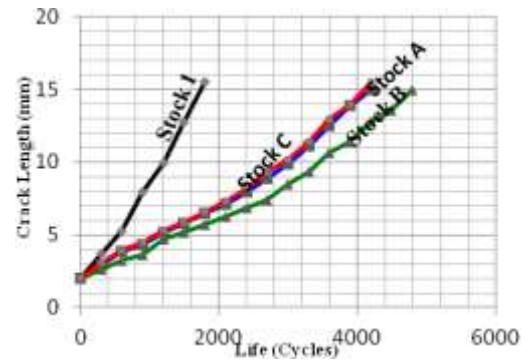


Figure (22): Crack Length vs. Life (H-L) Sequence.

Figures (23), (24), (25) and (26) shows the plot of fatigue crack growth rate FCG (da/dN) as a function of stress intensity factor range ΔK for the stocks 1, A, B and C respectively. Also figure (27) shows the final results for these stocks under (H-L) sequence.

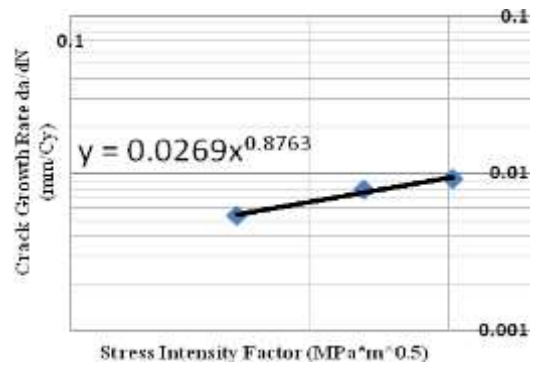


Figure (23): da/dN vs. ΔK , (Stock 1).

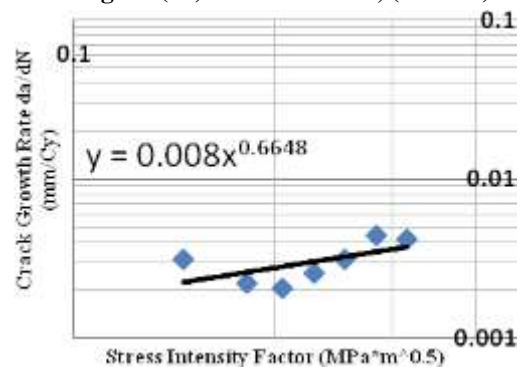


Figure (24): da/dN vs. ΔK , (Stock A).

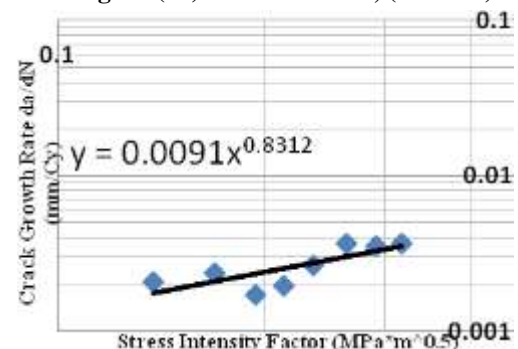


Figure (25): da/dN vs. ΔK , (Stock B).

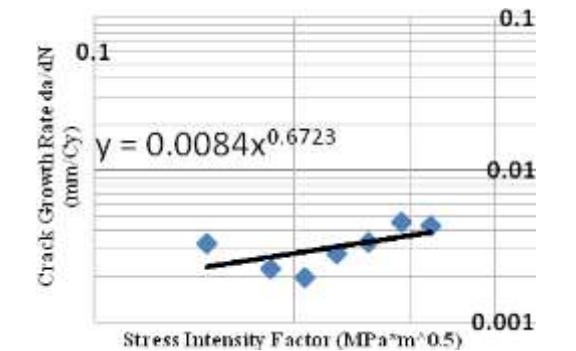


Figure (26): da/dN vs. ΔK , (Stock C).

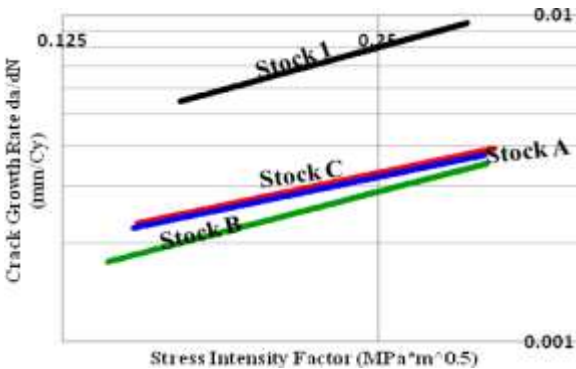


Figure (27): da/dN vs. ΔK , All Stock, at (H-L) Sequence. From the sets of experimental data, the values of the coefficient (A) and exponent (α) of these stocks in the Paris law takes the form:

stock 1 $\frac{da}{dN} = 26.9 \cdot 10^{-3} (\Delta K)^{0.876\alpha} \dots\dots (20)$

stock A $\frac{da}{dN} = 8 \cdot 10^{-3} (\Delta K)^{0.664\alpha} \dots\dots\dots (21)$

stock B $\frac{da}{dN} = 9.1 \cdot 10^{-3} (\Delta K)^{0.831\alpha} \dots\dots\dots (22)$

stock C $\frac{da}{dN} = 8.4 \cdot 10^{-3} (\Delta K)^{0.672\alpha} \dots\dots\dots (23)$

These results may be ascribed to the same reasons that mentioned previously with the same stocks under constant amplitude load where stock B was the best.

Table (7) shows the Miner life $N_{f_{Miner}}$, experimental life $N_{f_{exp}}$.

Table (7): Accumulative Fatigue Damage Results (H-L Sequence).

Stock	$N_f(Miner)$ (Cycle)	$N_f(exp.)$ (Cycle)
1	2857	1800
A	6000	4200
B	7368	4800
C	4714	4200

The experimental life results from the variable amplitude loading showed that at H-L sequence the results of Miner’s Rule were not acceptable in all results, where it seem not safe because the $N_{f_{Miner}}$ was larger than the $N_{f_{exp}}$. The results in (H-L) sequence far-away from the experimental results and that lead to avoid Miner rule during work with this sequence in case of study the flexing fatigue.

The results in tables (6) and (7) may be ascribed to polymer type, filler type and dispersion, loading conditions in addition to environmental condition such as temperature.

Conclusion:

From the observations and results obtained, the following conclusions can be drawn:

1. The tear and tensile strength were improved due to the raising the NR percentage and the addition of BR_{cis} in sidewall recipes.
2. Stock B showed good behavior compared to the other stocks.
3. Paris law gave reasonable results for crack growth rate of all the rubber stocks.
4. Miner’s Rule has not acceptable results at variable amplitude loading at both (L-H) and (H-L) sequence during work with flexing fatigue.
5. The proposed model showed well agreement with the experimental results.

References:

[1] W. Mars and A. Fatemi, Fatigue Crack Nucleation and Growth in Filled Natural Rubber, 7th International Conference on Biaxial/ Multiaxial Fatigue and Fracture, Berlin, pp. 329-334, 2004.

[2] W. Mars and A. Fatemi, Fatigue Crack Nucleation and Growth in Filled Natural Rubber Subjected To Multiaxial Stress States, 7th International Conference on Biaxial/Multiaxial Fatigue and Fracture, Berlin, (2004), pp. 329-334

[3] W. Mars and A. Fatemi, Multiaxial Stress Effects on Fatigue Behavior of Filled Natural Rubber, International Journal of Fatigue 28 (2006) 521–529.

[4] W. V. Mars and A. Fatimi, Factors that Affect the Fatigue Life of Rubber: A Literature Survey, Journal of Rubber Chemistry and Technology, Vol. 77, No.3,(2004).

[5] Joseph Thomas South, Mechanical Properties and Durability of Natural Rubber Compounds and Composites, Thesis of Doctor of Philosophy in Materials Engineering Science, Virginia, (2001).

[6] R. Harbour, A. Fatemi, W. V. Mars, Fatigue Crack Growth of Rubber Under Variable Amplitude Loading, 9th International Congress, Atlanta, Georgia, Oral/Poster Reference: Ft242, (2006).

[7] Young-Wook Chang, Fatigue Crack Growth Behaviour of NR/EPDM Blends, Dep. of Chemical Eng., Hanyang University, Ansan 425-791, Korea, (2006).

[8] M. Rowlinson, C.R. Herd, G. Moninot, N. Thomas and J.A. Ayala, The Effect of Carbon Black Morphological Characteristics on Tear Propagation In Rubbers, Bristol (UK) and Atlanta (USA), (2000).

[9] B. J Persson, O. Albohr, G. Heinrich And H. Ueba, Crack Propagation In Rubber-Like Materials, Institute of Physics Publishing Journal of Physics: Condensed Matter,J.Phys.: Condens. Matter 17 (2005) R1071–R1142, Germany, (2005). Doi:10.1088/0953-8984/17/44/R01.

[10] S. Kaang, Y. Woong Jin, Y. Huh, Wan-Jin Lee, Wan Bin, A Test Method to Measure Fatigue Crack Growth Rate of Rubbery Materials, South Korea, (2005). Doi:10.1016/J.Polymeresting.2005.12.005

[11] Alan N. Gent, Engineering with Rubber- How to Design Rubber Components, 2nd Ed., Hanser Publishers, Munich, Carl Hanser Verlag, chapter 5, (2001).

[12] Lake, G. J. and Clapson, B. E. Truck tire groove cracking, theory and practice. Rubber Chem. Tech., 44:1186-1202. (1971).

[13] Young, D. Application of Fatigue Methods Based on Fracture Mechanics for Tire Compound Development. Rubber Chem.Technol., 63:567-581. (1990).

[14] S. Kaang, C. Nah, Fatigue crack growth of double-networked natural rubber, Polymer 39 (11) (1998) 2209.

[15] D.G. Young, Fatigue Crack Propagation In Elastomer Compounds: Effects Of Strain Rate, Temperature, Strain Level, and Oxidation, Rubber Chem. Technol. 59 (1986) 809.

- [16] G.J. Lake, P.B. Lindley, Cut growth and Fatigue of Rubber. Part 2. Experiments on a Noncrystallizing Rubber, *J.Polym.Sci.8* (1964)707.
- [17] Young, D.G., Rubber Chemistry and Technology, 59, 809-825 (1986).
- [18] Lake, G.J and Lindley, P.B., Rubber Chemistry and Technology, 39, 348-364 (1966).
- [19] Prabhakar Soma, Naoya TADA, Makoto Uchida, Yoshifumi Taga, And Kazunari Nakahara, A Fracture Mechanics Approach For Evaluating The Effects Of Heat Aging On Fatigue Crack Growth Of Vulcanized Natural Rubber, Asian Pacific Conference For Materials And Mechanics, Yokohama, Japan, (2009).
- [20] Frank Abraham, The Influence of Minimum Stress on The Fatigue Life of Non Strain- Crystallising Elastomers, Ph.D. thesis, Coventry University in collaboration with the Deutsches Institut für Kautschuk technologie e.V., (2002).
- [21] Thomas A G "Rupture of rubber. V Cut growth in NR vulcanizates" *J Polym Sci*, **31**, 467-480 (1958).
- [22] Derham C J & Thomas AG "Creep under repeated stressing" *Rubber Chem Tech*, **50**, 397-401.(1977).
- [23] Lindley P B "Relation between hysteresis and the dynamic crack growth resistance of NR" *Int. J. Fracture*, **9**, 449-462 (1973)
- [24] Cadwell S M, Merrill R A, Slomani C M & Yost F L *Ind. & Eng. Chem*, **12**, 19 (1940).
- [25] Gdoutos, E. E., Fracure Mechanics – An Introduction, Kluwer Academic Publishers (1993).
- [26] P.M. Schuble, E.E. Gdoutos and I.M. Daniel, Fatigue Characterization of Tire Rubber, Robert McCormick School of Engineering and Applied Science, Northwestern University, Evanston IL 60208, (2002).
- [27] Ioannis Papadopoulos, Predicting The Fatigue Life of Elastomer Components, Ph.D. Thesis, Dep. of Materials, Queen Mary, University of London, UK , (2005).
- [28] Busfield, J.J.C. "The Prediction of The Mechanical Performance of Elastomeric Components Using Finite Element Analysis," Ph.D. thesis, Queen Mary, U.of London. (2000).
- [29] Gang Liu, Characterization and Identification of Bituminous Materials Modified with Montmorillonite Nanoclay, Ph.D. Thesis, University of Technology Delft, China, 2011.
- [30] Ashok V. Kumar, Nam P. Suh, Nagaraj K. Arakere and Nam Ho Kim, Engineering Design, CRC Press LLC., (2005).
- [31] Sun, A. N. Gent, P. Marteny, *Tire Scince Technol.* 28, 196 (2000).
- [32] H. J.M. Al-Alkawi, D.S. Al-Fattal and Nabel Kadum Abd-Ali, Studying the Effect of Rubber Filled Carbon Black in Design of Truck Tires Sidewall Recipe, *Journal of Eng. and Tech.*, to be published, (2012).
- [33] ASTM D412, Vulcanized Rubber and Thermoplastic Elastomers-Tension, Annual Book of ASTM Standards, Vol. 09.01, (2003).
- [34] ASTM D 624, Tear Strength of Conventional Vulcanized Rubber, Annual Book of ASTM Standards, Vol. 09.01, (2001).
- [35] ASTM D 813, Rubber Deterioration-Crack Growth, Annual Book of ASTM Standards, Vol. 09.01, (2000).
- [36] ASTM D 430, Rubber Deterioration-Dynamic Fatigue, Annual Book of ASTM Standards, Vol. 09.01, (2000).
- [37] H. J.M. Al-Alkawi, D.S. Al-Fattal and Nabel Kadum Abd-Ali, An Experimental Study of The Effect of the Type of Carbon Black In the Design of Truck Tire Sidewall Recipe, Conference of Technical College, Najaf-Iraq, (2012).
- [38] Charles A. Harper, Handbook of Plastics Elastomers and Composites, 4th Ed., McGraw-Hill Handbooks; (www.digitalengineeringlibrary.com), (2004).
- [39] Alan N. Gent, "Engineering with Rubber- How to Design Rubber Components", 2nd Ed., Hanser Publishers, Munich, (2001).
- [40] M.T. Shaw and W.J. MacKnight, Introduction to Polymer Viscoelasticity, Published by John Wiley & Sons, Inc., Hoboken, New Jersey, 3rd Ed., (2005).
- [41] R.K. Matthan, Rubber Engineering, Indian Rubber Institute, Tata McGraw-Hill Publishing Co. Ltd., New Delhi, (1998).
- [42] Sadhan K. De and Jim R. White, Rubber Technologist's Handbook, Rapra Technology Limited, U K , (2001).
- [43] Klaus Friedrich, Stoyko Fakirov and Zhong Zhang, "Polymer Composites From Nano-to Macro-Scale", Springer Science and Business Media Inc., (2005).
- [44] Mathias Brieu, J. Diani, C. Mignot and C. Moriceau, "Response of a Carbon Black Filled SBR under Large Strain Cyclic Uniaxial Tension", *International Journal of Fatigue* 32, Doi:10.1016/ijfatigue.2010.06.002. Elsevier LTD, (2010).
- [45] Lake G.J and Lindley P.B., Ozone cracking, flex cracking and fatigue of rubber, *Rubber J.* Vol.146, No.10, (1964). p.24.
- [46] Bathias C., Legorju-Jago K. "Fatigue Initiation and Propagation in Natural and Synthetic Rubbers," Presented at the 2nd International Conference on Fatigue, Williamsburg, VA, (2000).
- [47] W.V. Mars, A. Fatemi, A literature Survey on Fatigue Analysis Approaches for Rubber, *International Journal of Fatigue* 24, 949–961, 2002.
- [48] Abass. A. Al-Asadee, Studying the Mechanical Properties of Rubber Under The Effect of Constant and Variable Amplitude Fatigue Stresses, Ph.D. thesis, Uni. of Tech., Iraq, (2008).